

Phase diagrams of polydisperse van der Waals fluids

L. Bellier-Castella[†], H. Xu[†] and M. Baus^{††}

[†] Département de Physique des Matériaux (UMR 5586 du CNRS),
Université Claude Bernard-Lyon1, 69622 Villeurbanne Cedex, France

^{††} Physique des Polymères, Université Libre de Bruxelles,
Campus Plaine, CP 223, B-1050 Brussels, Belgium

PACS numbers: 05.70.Fh, 64.70.Fx, 82.70.Dd

Abstract

The phase behavior of a system composed of spherical particles with a monomodal size distribution is investigated theoretically within the context of the van der Waals approximation for polydisperse fluids. It is shown how the binodals, spinodals, cloud-point and shadow curves as well as all the (polydispersity induced) critical points can be obtained for a variety of interaction potentials. The polydispersity induced modifications of the phase diagram (even for a polydispersity index I as small as $I \approx 1.01$) should be observable in some colloidal dispersions.

I. INTRODUCTION

Many of the systems encountered in soft-matter physics (such as e.g. colloidal dispersions¹, liquid crystals², polymeric melts³) are fluids exhibiting one or several “polydispersities” because, by the very nature of their production process, these fluids are collections of complex molecular objects which are not strictly identical one to another. When these objects can be grouped into n sets of identical objects they form an ordinary n -component mixture⁴ whereas here we will focus instead on the case where the differences between these objects (e.g. differences in size, shape, surface charge, chemical composition, etc.) are distributed in an almost continuous manner in which case they can be described as “continuous” mixtures containing infinitely many components⁵. In the present study we will consider one of the simplest situations where the system is composed of spherical molecular objects which differ only in size. This excludes the liquid crystals and polymeric melts from our consideration. We will hence focus our attention on colloidal dispersions of spherical particles with a continuous size distribution⁶. In practice, this size distribution can be either monomodal (i.e. having only one maximum) or multimodal (i.e. having several maxima). We will again consider only the simplest case of a system with a monomodal size distribution⁶. Such systems can hence be considered as polydisperse generalizations of single component systems (whereas systems with a multimodal size distribution are generalizations of multi-component mixtures). When this monomodal size distribution is strongly peaked around its maximum one often refers to the corresponding colloidal dispersion as being monodisperse⁷. At present, such monodisperse colloidal dispersions are often used as testing ground for the study of various aspects of liquid state theory⁷. Indeed, by clever chemical engineering the colloidal particles can often be endowed with properties which are outside the range of ordinary single component systems (e.g. they can be prepared such as to have hard-sphere like repulsions and short-range attractions⁷). Nevertheless, even in those colloidal dispersions which are usually denoted as monodisperse there always remains

a residual size distribution. While the influence of this (unavoidable) polydispersity on the behavior of a single phase is well understood⁸, the first-principles study of its influence on a phase separation process is on the contrary still under active scrutiny⁹. Because the theoretical study of phase separations in polydisperse systems is faced with rather heavy technical problems we will consider here only the simplest possible phase separation, namely a fluid-fluid phase transition⁴. The theoretical tool used to describe this transition will again be the simplest one, namely the van der Waals (vdW) approximation¹⁰. It is indeed well known that the vdW-approximation provides us with a description of the phase separation of a fluid into a dilute fluid (or gas phase) and a dense fluid (or liquid phase) which is both simple and physically sound. It moreover involves a (mean-field) critical point which constitutes an important feature of many phase diagrams⁴. The vdW-approximation is also very robust and can be generalized in several ways, including for polydisperse systems^{11,12}. In the present study we will therefore focus our attention on the modifications brought about by the polydispersity to the binodal and critical point of a vdW-fluid with a monomodal size distribution. Such a description will of course not always be fully realistic for a given colloidal dispersion but we may hope that it retains the qualitative correctness which has characterized the widespread use of vdW-like descriptions in the past¹⁰. Since the present vdW-approximation is restricted to fluid phases only it will not be possible here to sort out which parts of the phase diagrams obtained are metastable with respect to the solid phases. By focusing on the fluid phases only, we are nevertheless able to show how the many technical problems raised by the study of phase equilibria in polydisperse systems can be solved, paving hereby the way for their later extensions to other phases and more involved descriptions.

In section II we summarize the thermodynamic conditions of phase coexistence in a polydisperse system in terms of the system's free-energy^{4,5} which has here to be viewed as a functional of the density distribution among the species. We also deduce the thermodynamic stability conditions of a polydisperse system from the convexity of this free-energy functional. This procedure, which is intrinsic in the sense that it does not rely on taking the limit

of an infinitely many component system is, as far as we are aware, new. In section III we introduce the vdW free-energy in a form already used elsewhere¹² (for the study of weakly polydisperse systems) except that here we include the cases where the polydispersity also affects the amplitude of the interaction potential. The monomodal parent phase size distributions considered in this work are introduced in section IV while section V is devoted to the solution method to be used subsequently for obtaining the numerical solutions of the integral equations which, for a polydisperse system, replace the algebraic equations governing the phase equilibria. This method can be generalized to any system for which the free-energy has an excess (over ideal) part which depends on a finite number of (generalized) moments of the polydispersity distribution. In section VI we show how the thermodynamic stability conditions of section II can be reduced to closed algebraic equations whenever the excess free-energy is of this particular type. In section VII we present explicit phase diagrams for interaction potentials with and without amplitude polydispersity. The critical behavior of a polydisperse vdW fluid is studied further in section VIII while the final section IX contains our conclusions.

II. PHASE EQUILIBRIUM IN A POLYDISPERSE FLUID

The statistical mechanical description of a polydisperse equilibrium system¹² is equivalent to a density functional theory for a system whose number density, say $\rho(\mathbf{r}, \sigma)$, depends besides the position variable \mathbf{r} (assuming spherical particles) moreover on a continuous species label σ (considered to be dimensionless). Such a theory is completely determined by the knowledge of its intrinsic Helmholtz free-energy (F) per unit volume (V), $f = F/V$, which is a function of the temperature (T) and a functional of the number density, $f = f(T, [\rho])$, where $[\rho]$ indicates a functional dependence on $\rho(\mathbf{r}, \sigma)$. All thermodynamic properties can then be deduced from $f(T, [\rho])$ by functional differentiation¹³. Below we will consider only (uniform and isotropic) fluid phases for which $\rho(\mathbf{r}, \sigma)$ is independent of \mathbf{r} , hence $\rho(\mathbf{r}, \sigma) \equiv \rho(\sigma)$.

A. The thermodynamic functionals

The phase behavior of a polydisperse fluid is determined by the chemical potential of the various species σ , $\mu = \mu(\sigma, T, [\rho])$, and the pressure, $p = p(T, [\rho])$, of the system. These functionals can be obtained from $f(T, [\rho])$ by the usual rules¹³, suitably extended to a continuous mixture⁵, as:

$$\mu(\sigma, T, [\rho]) = \delta f(T, [\rho]) / \delta \rho(\sigma) ; \quad (1)$$

$$p(T, [\rho]) = \int d\sigma \rho(\sigma) \mu(\sigma, T, [\rho]) - f(T, [\rho]) . \quad (2)$$

In what follows it will be convenient to split these quantities into an explicitly known ideal gaz part (*id*) and a generally unknown excess part (*ex*), for ex. $f = f_{id} + f_{ex}$, with:

$$f_{id}(T, [\rho]) = k_B T \int d\sigma \rho(\sigma) \left\{ \ln \left(\Lambda^3(\sigma) \rho(\sigma) \right) - 1 \right\} \quad (3)$$

$$\mu_{id}(\sigma, T, [\rho]) = k_B T \ln \left\{ \Lambda^3(\sigma) \rho(\sigma) \right\} \quad (4)$$

$$p_{id}(T, [\rho]) = k_B T \int d\sigma \rho(\sigma) \quad (5)$$

where k_B denotes Boltzmann's constant, $\Lambda(\sigma)$ the thermal de Broglie wavelength of species σ , and the integrals over σ extend over the whole domain of definition of $\rho(\sigma)$.

B. Phase coexistence conditions

When for a given T , a parent phase of density $\rho_0(\sigma)$, phase separates into n daughter phases of density $\rho_i(\sigma)$ ($i = 1, \dots, n$), the thermodynamic conditions of phase equilibrium⁴ imply the equality of the pressures:

$$p(T, [\rho_1]) = p(T, [\rho_2]) = \dots = p(T, [\rho_n]) \quad (6)$$

and of the chemical potentials:

$$\mu(\sigma, T, [\rho_1]) = \mu(\sigma, T, [\rho_2]) = \dots = \mu(\sigma, T, [\rho_n]) \quad (7)$$

for each species σ . It will be convenient to rewrite, $\rho_j(\sigma) = \rho_j h_j(\sigma)$, where $\rho_j = \int d\sigma \rho_j(\sigma)$ is the average density and $h_j(\sigma)$ the normalized (viz. $\int d\sigma h_j(\sigma) = 1$) polydispersity distribution of phase j ($j = 0, 1, 2, \dots, n$). The phase separation is moreover constrained by the conservation of the total number of particles of each species σ :

$$h_0(\sigma) = \sum_{i=1}^n x_i h_i(\sigma) \quad (8)$$

where, $x_i = N_i/N_0$, is the ratio of the total number of particles (N_i) in phase i to the total number of particles in the parent phase (N_0). Moreover, the conservation of the total volume occupied by the parent phase can be written:

$$v_0 = \sum_{i=1}^n x_i v_i \quad (9)$$

where $v_j = 1/\rho_j$ ($j = 0, 1, 2, \dots, n$). Finally, the normalization of the $h_j(\sigma)$ in (8) implies:

$$1 = \sum_{i=1}^n x_i \quad (10)$$

which expresses the conservation of the total number of particles.

In principle, given T , ρ_0 and $h_0(\sigma)$, one has to solve the system of equations (6-10) for the ρ_i and $h_i(\sigma)$ ($i = 1, 2, \dots, n$). Even when starting from a relatively simple $f(T, [\rho])$ this turns out to be a rather formidable task because (6-7) are no longer algebraic equations (as would be the case for ordinary mixtures) but become here integral equations for the $h_i(\sigma)$. In order to simplify the situation somewhat we will restrict ourselves here to two-phase coexistences only, i.e. to $n = 2$. In a polydisperse system n can in principle be arbitrarily large because the Gibbs phase rule⁴ does not restrict the value of n in a system of infinitely many species⁵. In practice, however, a polydisperse system does rarely use this infinite number of thermodynamic degrees of freedom. Since these multiple-phase coexistences are expected to occur at low temperatures, the restriction to two-phase coexistences ($n = 2$) implies that the value of T should be chosen high enough (see below). Note that this is

consistent with our earlier restriction (see above) to fluid phases because for low temperatures some of the (multiple) fluid phases may have to compete with some of the solid phases.

For a two-phase coexistence ($n = 2$) the number fractions x_i ($i = 1, 2$) can be obtained from (9-10) as:

$$x_1 = \frac{v_0 - v_2}{v_1 - v_2}, \quad x_2 = \frac{v_0 - v_1}{v_2 - v_1} \quad (11)$$

expressing the lever rule⁴, whereas $h_2(\sigma)$ can be eliminated by using moreover (8):

$$h_2(\sigma) = \frac{v_2 - v_1}{v_0 - v_1} h_0(\sigma) + \frac{v_2 - v_0}{v_1 - v_0} h_1(\sigma) \quad (12)$$

where $v_0 = 1/\rho_0$ and $h_0(\sigma)$ are given parent phase data. To find $v_1 = 1/\rho_1$, $v_2 = 1/\rho_2$ and $h_1(\sigma)$ we need three relations. To this end we use (4) to rewrite (7) for $n = 2$ as:

$$\rho_1(\sigma) = \rho_2(\sigma) \exp \{ \beta \Delta \mu_{ex}(\sigma, T, [\rho_1, \rho_2]) \} \quad (13)$$

where $\beta = 1/k_B T$ and :

$$\Delta \mu_{ex}(\sigma, T, [\rho_1, \rho_2]) = \mu_{ex}(\sigma, T, [\rho_2]) - \mu_{ex}(\sigma, T, [\rho_1]) \quad (14)$$

with μ_{ex} being the excess part of $\mu(\sigma, T, [\rho])$. In terms of the $h_i(\sigma)$, eq. (13) becomes:

$$h_1(\sigma) = h_2(\sigma) A_{12}(\sigma, T; \rho_1, \rho_2; [h_1], [h_2]) \quad (15)$$

where A_{12} is a shorthand notation for $A_{12} = (v_1/v_2) \exp\{\beta \Delta \mu_{ex}\}$. Eliminating $h_2(\sigma)$ from (15) by using (12) one obtains finally:

$$h_1(\sigma) = h_0(\sigma) H(\sigma, T; \rho_0, \rho_1, \rho_2; [h_1], [h_0]) \quad (16)$$

where, $H = (v_2 - v_1) A_{12} / \{ (v_0 - v_1) + (v_2 - v_0) A_{12} \}$, and it is understood that $h_2(\sigma)$ has also been eliminated from A_{12} by using (12). Eq. (16) is our first relation between ρ_1 , ρ_2 and $h_1(\sigma)$. Given T , ρ_0 and $h_0(\sigma)$, eq. (16) can in principle be solved with respect to $h_1(\sigma)$ for given ρ_1 and ρ_2 values. A first relation between ρ_1 and ρ_2 can then be found by solving moreover:

$$1 = \int d\sigma h_0(\sigma) H(\sigma, T; \rho_0, \rho_1, \rho_2; [h_1], [h_0]) \quad (17)$$

which follows from (16) and the normalization of $h_1(\sigma)$. Finally, the system of equations is closed by solving moreover (6):

$$p(T, [\rho_1]) = p(T, [\rho_2]) \quad (18)$$

expressing the equality of the pressures. It is obvious that solving a (two-phase) coexistence problem for a polydisperse fluid is much more involved than the corresponding problem for a monodisperse (single species) fluid. This is due mainly to the central integral equation (16) which governs the change in the polydispersity or species distribution between the parent phase and the two coexisting phases (cf (12)), a process usually called fractionation⁹. The extension of (16-18) for the case of a n -phase coexistence is straightforward.

C. Thermodynamic stability conditions

Of course, not for every prescribed $\{T, \rho_0(\sigma)\}$ will the corresponding phases exist or be thermodynamically stable. For this to be the case, the free-energy density, $f(T, [\rho])$, must remain a convex functional of $\rho(\sigma) = \rho_0(\sigma)$, i.e. it must satisfy:

$$f(T, [\rho + \lambda\delta\rho]) < \lambda f(T, [\rho + \delta\rho]) + (1 - \lambda)f(T, [\rho]) \quad (19)$$

for any, $0 < \lambda < 1$, and for any change, $\delta\rho(\sigma) \neq 0$, of the functional form of $\rho(\sigma)$. If we consider only infinitesimal changes, $\delta\rho(\sigma)$, eq. (19) is equivalent to:

$$0 < \sum_{k=2}^{\infty} \frac{1}{k!} (\lambda - \lambda^k) \delta^k f(T, [\rho]) \quad (20)$$

where $\delta^k f$ is the k -th functional variation of f :

$$\delta^k f = \int d\sigma_1 \dots \int d\sigma_k K_k(\sigma_1, \dots, \sigma_k; T, [\rho]) \delta\rho(\sigma_1) \dots \delta\rho(\sigma_k) \quad (21)$$

and K_k is an integral operator whose kernel is :

$$K_k(\sigma_1, \dots, \sigma_k; T, [\rho]) = \frac{\delta^k f(T, [\rho])}{\delta\rho(\sigma_1) \dots \delta\rho(\sigma_k)} . \quad (22)$$

Hence, the condition for stability with respect to infinitesimal changes ($\rho(\sigma) \rightarrow \rho(\sigma) + \delta\rho(\sigma)$) reduces ($\delta^{k+1}f \ll \delta^k f$) to:

$$0 < \delta^2 f(T, [\rho]). \quad (23)$$

In a case of marginal stability there must exist at least one “fluctuation” $\delta\rho(\sigma) \neq 0$, say $\delta\rho_0(\sigma)$, such that $\delta^2 f(T, [\rho]) = 0$, or explicitly:

$$\int d\sigma_1 \int d\sigma_2 K_2(\sigma_1, \sigma_2; T, [\rho]) \delta\rho_0(\sigma_1) \delta\rho_0(\sigma_2) = 0 \quad (24)$$

for a given T and $\rho(\sigma)$. Any solution $\delta\rho_0(\sigma)$ of (24) will be called a critical fluctuation. For the system to remain stable with respect to these critical fluctuations $\delta\rho_0(\sigma)$ we must have according to (20), $\delta^3 f = 0$ (because the sign of $\delta^3 f$ changes with the sign of $\delta\rho_0(\sigma)$ while (24) does not fix the sign of $\delta\rho_0(\sigma)$) and $\delta^4 f > 0$:

$$\int d\sigma_1 \int d\sigma_2 \int d\sigma_3 K_3(\sigma_1, \sigma_2, \sigma_3; T, [\rho]) \delta\rho_0(\sigma_1) \delta\rho_0(\sigma_2) \delta\rho_0(\sigma_3) = 0; \quad (25)$$

$$\int d\sigma_1 \int d\sigma_2 \int d\sigma_3 \int d\sigma_4 K_4(\sigma_1, \sigma_2, \sigma_3, \sigma_4; T, [\rho]) \delta\rho_0(\sigma_1) \delta\rho_0(\sigma_2) \delta\rho_0(\sigma_3) \delta\rho_0(\sigma_4) > 0. \quad (26)$$

Note that in the present context the stability conditions (23-26) imply stability with respect to changes in both the average density ($\delta\rho(\sigma) = \delta\rho h(\sigma)$) and the composition ($\delta\rho(\sigma) = \rho \delta h(\sigma)$). The values of T and $\rho(\sigma)$ for which (24) has a solution define a (generalized or polydisperse) spinodal whereas those values for which (24) and (25-26) are simultaneously satisfied correspond to the critical states of the polydisperse fluid. For a monodisperse fluid these conditions reduce to well known results but for a polydisperse fluid they are much less well known and also much more difficult to study. For instance, for eq. (24) to have a solution, the Fredholm determinant¹⁴ of the integral operator K_2 must vanish. This functional determinant however is equivalent to an infinite series of ordinary determinants¹⁴. As shown by Kincaid et al.¹⁵, in order to draw any conclusion from such a series of determinants one must have at its disposal a smallness parameter allowing one to truncate this series. For

the weakly polydisperse fluids considered by Kincaid et al.¹⁵ there is such a parameter but for the strongly polydisperse systems to be considered here there is none. Needless to say that in order to make progress we will need further simplifying assumptions. To this end we will introduce in the next section a model expression for $f(T, [\rho])$ which is simple enough to allow us to tackle the various technical problems encountered above in the study of phase equilibria in polydisperse fluids.

III. THE POLYDISPERSE VAN DER WAALS FLUID

An explicit expression for $f(T, [\rho])$, which is both relatively simple and physically sound, can be obtained from the van der Waals (vdW) theory¹⁰. For a polydisperse fluid the vdW free-energy reads^{11,12}:

$$f(T, [\rho]) = k_B T \int d\sigma \rho(\sigma) \left\{ \ln \left(\frac{\Lambda^3(\sigma) \rho(\sigma)}{E[\rho]} \right) - 1 \right\} + \frac{1}{2} \int d\sigma \int d\sigma' V(\sigma, \sigma') \rho(\sigma) \rho(\sigma') \quad (27)$$

where the hard repulsions between the particles are taken into account via the usual vdW excluded volume correction¹⁰, $E[\rho]$:

$$E[\rho] = 1 - \int d\sigma v(\sigma) \rho(\sigma) \quad (28)$$

$v(\sigma)$ being the volume of a particle of species σ , while the cohesion energy¹⁰ resulting from the interparticle attractions described by $V_A(r; \sigma, \sigma')$ is given in the vdW mean field approximation by the second term of (27) with:

$$V(\sigma, \sigma') = \int d\mathbf{r} V_A(r; \sigma, \sigma'). \quad (29)$$

From (27) and (1) we obtain:

$$\mu(\sigma, T, [\rho]) = k_B T \ln \left\{ \frac{\Lambda^3(\sigma) \rho(\sigma)}{E[\rho]} \right\} + k_B T \frac{v(\sigma)}{E[\rho]} \int d\sigma' \rho(\sigma') + \int d\sigma' V(\sigma, \sigma') \rho(\sigma') \quad (30)$$

while (2) yields:

$$p(T, [\rho]) = \frac{k_B T}{E[\rho]} \int d\sigma \rho(\sigma) + \frac{1}{2} \int d\sigma \int d\sigma' V(\sigma, \sigma') \rho(\sigma) \rho(\sigma'). \quad (31)$$

If $D(\sigma, \sigma')$ denotes the contact distance between two particles of species σ and σ' , we have $V_A(r; \sigma, \sigma') = 0$ when $r < D(\sigma, \sigma')$ so that (29) can always be rewritten^{10,12}:

$$V(\sigma, \sigma') = -\epsilon(\sigma, \sigma') \frac{4\pi}{3} (D(\sigma, \sigma'))^3 \quad (32)$$

where $\epsilon(\sigma, \sigma') > 0$ characterizes the amplitude of the attractions. For simplicity we will use the Lorentz-Berthelot mixing rules^{4,8}:

$$\begin{aligned} D(\sigma, \sigma') &= \{D(\sigma, \sigma) + D(\sigma', \sigma')\}/2 \\ \epsilon(\sigma, \sigma') &= \{\epsilon(\sigma, \sigma)\epsilon(\sigma', \sigma')\}^{1/2} \end{aligned} \quad (33)$$

together with the additivity assumption, $D(\sigma, \sigma) = 2R(\sigma)$, $R(\sigma)$ being the radius of a particle of species σ , so that $v(\sigma) = (4\pi/3)R^3(\sigma)$. Choosing $\sigma = 1$ as a reference species we may use $R(1)$ as length scale and $\epsilon(1, 1)$ as energy scale. Our basic (dimensionless) polydispersity variable will hence be, $R(\sigma)/R(1)$, which will be denoted here, $\sigma = R(\sigma)/R(1)$, so that σ denotes here both a species and its associated polydispersity variable, $R(\sigma)/R(1)$. Below it will be convenient to consider various particular cases of (32-33) by introducing two indices, $0 \leq l \leq 1$ and $0 \leq n \leq 1$, and rewrite $D(\sigma, \sigma) = \sigma^n D(1, 1)$, $v(\sigma) = \sigma^{3n} v(1)$, $\epsilon(\sigma, \sigma) = \sigma^{2l} \epsilon(1, 1)$ so that $\{l = 0, n = 0\}$ corresponds to the absence of polydispersity, $\{l = 1, n = 0\}$ to polydispersity of the amplitude or interaction strength only, $\{l = 0, n = 1\}$ polydispersity in size only, while $\{l = 1, n = 1\}$ corresponds to both amplitude and size polydispersity. Note that the amplitude polydispersity¹⁶ ($l \neq 0$) includes the polydispersity which originates from the species dependence of the range of the interaction potential ($V_A(r; \sigma, \sigma')$). Finally, the present vdW-model is only a particular case of the general class of models considered by Gualtieri et al¹¹. It has, however, the advantage that it can be easily related to a realistic interaction potential via Eqs. (29) and (32).

IV. THE PARENT PHASE DISTRIBUTION

To complete the description of our system we shall now specify, $\rho_0(\sigma) = \rho_0 h_0(\sigma)$, the distribution of the parent phases to be considered here. The polydispersity distribution $h_0(\sigma)$ is constrained by the fact that it must be non-negative and normalized. We will assume moreover that the values of $\sigma = R(\sigma)/R(1)$ are distributed continuously within $0 < \sigma < \infty$. Of course, very large values of σ are unphysical but these will be given a very small weight by requiring that $h_0(\sigma)$ decays with σ in a manner which is sufficiently rapid for all the moments of $h_0(\sigma)$, $m_k^{(0)} = \int_0^\infty d\sigma \sigma^k h_0(\sigma)$, to exist. Moreover, we will restrict ourselves to monomodal distributions⁶ so that the systems considered here are polydisperse generalizations of single component systems. Two often used candidates^{3,6} are the Schulz-Zimm (SZ) distribution, $h_0^{(SZ)}(\sigma) = c \sigma^a \exp(-b\sigma)$, and the log-normal (LN) distribution, $h_0^{(LN)}(\sigma) = c \exp\{-a (\ln(\sigma/b))^2\}$. In each case the parameters $\{a, b, c\}$ are determined by the normalization ($m_0^{(0)} = 1$), the mean value ($m_1^{(0)}$) and the polydispersity index, $I = m_2^{(0)}/(m_1^{(0)})^2$, of the distribution. In what follows we will take $m_1^{(0)} = 1$ so that the size of the reference species, $R(1)$, is equal to the average value of $R(\sigma)$ in the parent phase distribution. Under these circumstances the SZ distribution can be written:

$$h_0^{(SZ)}(\sigma) = \frac{\alpha^\alpha}{\Gamma(\alpha)} \cdot \sigma^{\alpha-1} \cdot \exp(-\alpha\sigma) \quad (34)$$

where $\Gamma(\alpha)$ is the Euler gamma function of argument $0 < \alpha < \infty$, a parameter which determines the inverse width of the SZ distribution, or equivalently, its polydispersity index, $I^{(SZ)} = 1 + 1/\alpha$. The moments of (34) are given by:

$$m_k^{(SZ)} = \frac{1}{\alpha^k} \frac{\Gamma(\alpha + k)}{\Gamma(\alpha)} \quad (35)$$

which, when k is an integer, can be rewritten (for $k \geq 2$) as:

$$m_k^{(SZ)} = \prod_{n=1}^{k-1} \left(1 + \frac{n}{\alpha}\right). \quad (36)$$

For the LN distribution we have similarly:

$$h_0^{(LN)}(\sigma) = \frac{I}{(2\pi \ln I)^{1/2}} \cdot \exp \left\{ -\frac{\ln^2[I^{3/2} \sigma]}{2 \ln I} \right\} \quad (37)$$

where $I^{(LN)} = I$ while the moments of (37) are given by:

$$m_k^{(LN)} = I^{k(k-1)/2}. \quad (38)$$

In both cases we have hence $m_0^{(0)} = m_1^{(0)} = 1$ and $m_2^{(0)} = I = 1 + 1/\alpha$. Note that in the monodisperse limit, ($I \rightarrow 1$ or $\alpha \rightarrow \infty$) both these distributions reduce to the Dirac distribution, $\delta(\sigma - 1)$, centered on the reference species ($\sigma = 1$). On the contrary, when I becomes very large ($I \gg 1$) the above distributions become very wide, increasing hereby the importance of the larger particles (see Fig.1). As stated above, the presence of very large particles is unphysical and a realistic situation should be described by distributions which strictly vanish for σ larger than some maximum value. To avoid such problems, below we will consider only values of I in the range $1 < I < 2$. For such values the results obtained from the full distributions will be similar to those obtained from the physically truncated distributions (with a slightly different I -value).

V. THE SOLUTION METHOD

In what follows it will be convenient to use dimensionless variables. Using $\epsilon(1, 1)$ as energy scale and $R(1)$ as length scale, $\sigma = 1$ being the reference species, we can introduce $t = k_B T/\epsilon(1, 1)$, $\bar{\mu} = \mu/\epsilon(1, 1)$ as reduced temperature and chemical potential while, if $v(1) = \frac{4\pi}{3} R^3(1)$ represents the volume of the reference particle, for the reduced free-energy, pressure and average density we will use, respectively, $\bar{f} = f v(1)/\epsilon(1, 1)$, $\bar{p} = p v(1)/\epsilon(1, 1)$, $\eta = \rho v(1)$. The generalized moments ($m_k(\sigma) = \sigma^k$ but k need not be an integer) of the polydispersity distribution $h(\sigma)$ will be written:

$$m_k[h] = \int_0^\infty d\sigma m_k(\sigma) h(\sigma) \quad (39)$$

or, shortly, $m_k = m_k[h]$ for a general distribution $h(\sigma)$ and $m_k^{(j)} = m_k[h_j]$ when $h_j(\sigma)$ represents the distribution of phase j ($j = 0, 1, 2$). Finally, as explained at the end of section III, $V(\sigma, \sigma')$ will be written:

$$V(\sigma, \sigma') = V(1, 1)(\sigma \sigma')^l \left(\frac{\sigma^n + \sigma'^n}{2} \right)^3 \quad (40)$$

with $V(1, 1) = -8 \epsilon(1, 1)v(1)$, where the value of l controls the amplitude polydispersity while the value of n controls the size polydispersity. In terms of these variables we can rewrite the excess part of eqs. (30), needed for (14), as:

$$\begin{aligned} \bar{\mu}_{ex}(\sigma, t, \eta, [h]) = & -t \ln(1 - \eta m_{3n}) + \frac{t\eta m_0 m_{3n}(\sigma)}{1 - \eta m_{3n}} \\ & - \eta \{m_{l+3n}(\sigma)m_l + 3m_{l+2n}(\sigma)m_{l+n} + 3m_{l+n}(\sigma)m_{l+2n} + m_l(\sigma)m_{l+3n}\} \end{aligned} \quad (41)$$

while (31) becomes:

$$\bar{p}(t, \eta, [h]) = \frac{t\eta m_0}{1 - \eta m_{3n}} - \eta^2 (m_l m_{l+3n} + 3 m_{l+n} m_{l+2n}) \quad (42)$$

where it is seen that because of the polynomial character of (40) these expressions involve only a finite number of moments m_k , $\{k = 0, 3n, l, l+n, l+2n, l+3n\}$. Note that the exact number of moments depends on the values of l and n (for ex. when $l = 0$, $k = \{0, l\}$ or $k = \{3n, l+3n\}$ represent one and the same moment, resp. $k = 0$ and $k = 3n$). In the present context we can thus rewrite (16) as:

$$h_1(\sigma) = h_0(\sigma) H(t, \eta_0, \eta_1, \eta_2; \{m_k(\sigma)\}, \{m_k^{(1)}\}, \{m_k^{(0)}\}) \quad (43)$$

where the $\{m_k^{(2)}\}$ have been eliminated in favor of $\{m_k^{(0)}\}$ and $\{m_k^{(1)}\}$ by using (12):

$$m_k^{(2)} = \frac{v_2 - v_1}{v_0 - v_1} m_k^{(0)} + \frac{v_2 - v_0}{v_1 - v_0} m_k^{(1)}. \quad (44)$$

Although eq. (43) can be solved directly, as was done in¹², here we will take advantage of the structure of (43) to transform this integral equation for $h_1(\sigma)$ into a set of moment relations¹¹:

$$m_{k'}^{(1)} = \int d\sigma m_{k'}(\sigma) h_0(\sigma) H(t, \eta_0, \eta_1, \eta_2; \{m_k(\sigma)\}, \{m_k^{(1)}\}, \{m_k^{(0)}\}) \quad (45)$$

where both k' and k run through the finite set of moments $\{0, 3n, l, l+n, l+2n, l+3n\}$.

Note that for $k' = 0$, eq. (45) corresponds to (17) while (18) becomes here:

$$\frac{t\eta_1 m_0^{(1)}}{1 - \eta_1 m_{3n}^{(1)}} - \eta_1^2(m_l^{(1)} m_{l+3n}^{(1)} + 3 m_{l+n}^{(1)} m_{l+2n}^{(1)}) = \frac{t\eta_2 m_0^{(2)}}{1 - \eta_2 m_{3n}^{(2)}} - \eta_2^2(m_l^{(2)} m_{l+3n}^{(2)} + 3 m_{l+n}^{(2)} m_{l+2n}^{(2)}) \quad (46)$$

together with the normalization condition $m_0^{(0)} = m_0^{(1)} = m_0^{(2)} = 1$. For any given t , η_0 and $h_0(\sigma)$ (from which the $m_k^{(0)}$ can be determined) the seven unknowns $\{\eta_1, \eta_2, m_{3n}^{(1)}, m_l^{(1)}, m_{l+n}^{(1)}, m_{l+2n}^{(1)}, m_{l+3n}^{(1)}\}$ can then be obtained by solving the system of seven equations (45) and (46) for $\{k' = 0, 3n, l, l+n, l+2n, l+3n\}$. When this result is substituted in (43) we obtain $h_1(\sigma)$ and from (12) we obtain then $h_2(\sigma)$. This then completely solves the two-phase coexistence problem for the present vdW-model. In the monodisperse limit we have $m_k^{(j)} = 1$, for all k and j values, and (45-46) reduce then to the usual vdW equations for the binodal of the reference species. To solve (45-46) we have used an iterative process by starting from an initial guess of the solution (usually the monodisperse case). When using moreover a globally convergent Newton-Raphson method¹⁷ a (convergent) solution of (45-46) can easily be obtained even close to the critical points. The latter can hence be determined directly from the binodals but they can also be obtained by alternative procedures. One such procedure which is based on the stability analysis of section II C will be detailed in the next section whereas here we will focus on an alternative procedure based on the determination of the so-called cloud-point (C) and shadow (S) curves. These curves provide envelopes for the binodals. They can be obtained from (45-46) by considering a situation of insipient phase separation whereby phase 1 is present only in infinitesimal amounts. Returning to section II B this situation is seen to correspond to $x_1 \rightarrow 0$ or $v_2 \rightarrow v_0$ with v_1 and v_2 finite. From (12) and (44) it is seen that this implies $h_2(\sigma) \rightarrow h_0(\sigma)$ and $m_k^{(2)} \rightarrow m_k^{(0)}$. These curves are hence solutions of (cf. (43,45-46)):

$$h_1(\sigma) = h_0(\sigma) A_{12}(t, \eta_0 = \eta_2, \eta_1; \{m_k(\sigma)\}, \{m_k^{(1)}\}, \{m_k^{(0)}\}) \quad (47)$$

$$m_{k'}^{(1)} = \int_0^\infty d\sigma m_{k'}(\sigma) h_0(\sigma) A_{12}(t, \eta_0 = \eta_2, \eta_1; \{m_k(\sigma)\}, \{m_k^{(1)}\}, \{m_k^{(0)}\}) \quad (48)$$

$$\frac{t\eta_1 m_0^{(1)}}{1 - \eta_1 m_{3n}^{(1)}} - \eta_1^2(m_l^{(1)} m_{l+3n}^{(1)} + 3 m_{l+n}^{(1)} m_{l+2n}^{(1)}) = \frac{t\eta_0 m_0^{(0)}}{1 - \eta_0 m_{3n}^{(0)}} - \eta_0^2(m_l^{(0)} m_{l+3n}^{(0)} + 3 m_{l+n}^{(0)} m_{l+2n}^{(0)}) \quad (49)$$

where we took moreover into account in (47-48) that, $H \rightarrow A_{12}$, when $v_2 \rightarrow v_0$ (cf. (15-16)). The solution to (47-49) corresponding to the majority phase 2 yields then the so-called C-curve while the solution for the minority phase 1 yields the S-curve.

VI. CRITICAL POINT ANALYSIS OF THE VDW FREE-ENERGY

As explained in section II C, a free-energy density $f(T, [\rho])$ will be globally stable if it remains a convex functional of $\rho(\sigma)$ for any change, $\rho(\sigma) \rightarrow \rho(\sigma) + \delta\rho(\sigma)$. It then must satisfy eq. (19). The same free-energy will be locally stable when (20) holds, i.e. when the first functional variation $\delta^k f(T, [\rho])$ of $f(T, [\rho])$ which is non-zero corresponds to an even value of $k \geq 2$. We then have $\{\delta^2 f > 0\}$ for a (ordinary) stable state; $\{\delta^2 f = 0, \delta^3 f = 0, \delta^4 f > 0\}$ for a (ordinary) critical state, $\{\delta^2 f = \delta^3 f = \delta^4 f = \delta^5 f = 0, \delta^6 f > 0\}$ for a tricritical state, etc. Here we will limit ourselves to the equations determining the ordinary critical states of the vdW free-energy of section III. From (27) and (22) we obtain ($\beta = 1/k_B T$; $\bar{v}(\sigma_n) = v(\sigma_n)/E[\rho]$):

$$\beta K_2(\sigma_1, \sigma_2; T, [\rho]) = \frac{\delta(\sigma_1 - \sigma_2)}{\rho(\sigma_1)} + \beta V(\sigma_1, \sigma_2) + [\bar{v}(\sigma_1) + \bar{v}(\sigma_2)] + \rho \bar{v}(\sigma_1) \bar{v}(\sigma_2) \quad (50)$$

$$\begin{aligned} \beta K_3(\sigma_1, \sigma_2, \sigma_3; T, [\rho]) = & -\frac{\delta(\sigma_1 - \sigma_2)\delta(\sigma_2 - \sigma_3)}{\rho(\sigma_1)\rho(\sigma_2)} + 2\rho \bar{v}(\sigma_1) \bar{v}(\sigma_2) \bar{v}(\sigma_3) \\ & + [\bar{v}(\sigma_1) \bar{v}(\sigma_2) + \bar{v}(\sigma_2) \bar{v}(\sigma_3) + \bar{v}(\sigma_3) \bar{v}(\sigma_1)] \end{aligned} \quad (51)$$

$$\begin{aligned} \beta K_4(\sigma_1, \sigma_2, \sigma_3, \sigma_4; T, [\rho]) = & 2\frac{\delta(\sigma_1 - \sigma_2)}{\rho(\sigma_1)} \frac{\delta(\sigma_2 - \sigma_3)}{\rho(\sigma_2)} \frac{\delta(\sigma_3 - \sigma_4)}{\rho(\sigma_3)} \\ & + 6\rho \bar{v}(\sigma_1) \bar{v}(\sigma_2) \bar{v}(\sigma_3) \bar{v}(\sigma_4) + 2 [\bar{v}(\sigma_1) \bar{v}(\sigma_2) \bar{v}(\sigma_3) + \bar{v}(\sigma_1) \bar{v}(\sigma_2) \bar{v}(\sigma_4) \\ & + \bar{v}(\sigma_1) \bar{v}(\sigma_3) \bar{v}(\sigma_4) + \bar{v}(\sigma_2) \bar{v}(\sigma_3) \bar{v}(\sigma_4)] \end{aligned} \quad (52)$$

where it is seen that K_4 is positive definite while K_3 and K_2 can vanish because the volume $v(\sigma)$ of species σ and $E[\rho]$ of (28) are positive while $V(\sigma_1, \sigma_2)$ of (32) is negative. We now turn to eq. (24) which can be cast into an eigenvalue form^{15,18} by rewriting $\delta\rho(\sigma)$ as $\delta\rho(\sigma) = \rho(\sigma) \cdot e(\sigma)$ where $\rho(\sigma) = \rho h(\sigma)$ and $e(\sigma)$ is as yet unknown. Using moreover the dimensionless variables introduced in section V we can recast (24) and (50) in the form:

$$\int d\sigma_1 d\sigma_2 e(\sigma_1) \{ (h(\sigma_1)h(\sigma_2))^{1/2} \delta(\sigma_1 - \sigma_2) + h(\sigma_1) C_2(\sigma_1, \sigma_2; t, \eta) h(\sigma_2) \} e(\sigma_2) = 0 \quad (53)$$

where:

$$\begin{aligned} C_2(\sigma_1, \sigma_2; t, \eta) = & A (m_{3n}(\sigma_1)m_0(\sigma_2) + m_0(\sigma_1)m_{3n}(\sigma_2)) + A^2 m_{3n}(\sigma_1) m_{3n}(\sigma_2) \\ & - B \{ m_{l+3n}(\sigma_1)m_l(\sigma_2) + 3m_{l+2n}(\sigma_1)m_{l+n}(\sigma_2) \\ & + 3m_{l+n}(\sigma_1)m_{l+2n}(\sigma_2) + m_l(\sigma_1)m_{l+3n}(\sigma_2) \} \end{aligned} \quad (54)$$

together with the shorthand notations, $A = \eta/(1 - \eta m_{3n})$, and $B = \eta/t$. For convenience we rewrite (54) briefly as:

$$C_2(\sigma_1, \sigma_2; t, \eta) = \sum_{k, k'} c_{kk'}(t, \eta) m_k(\sigma_1) m_{k'}(\sigma_2) \quad (55)$$

where the $c_{kk'}$ can be deduced by identification of (55) with (54). From (55) it is obvious that $C_2(\sigma_1, \sigma_2; t, \eta)$ is completely embedded in the subspace spanned by the vdW-moments $\{m_k(\sigma); k = 0, 3n, l, l+n, l+2n, l+3n\}$. To solve (53) it will hence be sufficient to restrict $e(\sigma)$ to the same subspace¹⁸, i.e. $e(\sigma) = \sum_k e_k m_k(\sigma)$. A solution of the homogeneous equation (53) will hence exist provided the determinant of the matrix, $\underline{\underline{M}} + \underline{\underline{M}} \cdot \underline{\underline{C}} \cdot \underline{\underline{M}}$ vanishes. We can rewrite this matrix as $\underline{\underline{M}} \cdot \underline{\underline{A}}$, with $\underline{\underline{A}} = \underline{\underline{I}} + \underline{\underline{B}}$ and $\underline{\underline{B}} = \underline{\underline{C}} \cdot \underline{\underline{M}}$. Here, $I_{kk'} = \delta_{kk'}^{Kr}$ is the unit matrix, $C_{kk'} = c_{kk'}(t, \eta)$ the matrix of coefficients of (55), and $M_{kk'} = m_{k+k'}(\sigma)$ a matrix involving the moments of $h(\sigma)$. (Note that $m_k(\sigma)m_{k'}(\sigma) = m_{k+k'}(\sigma)$). Since $\det|M_{kk'}| \neq 0$, the equation of the spinodal (SP) can be written in various forms, e.g. :

$$\det|I_{kk'} + B_{kk'}| = 0, \quad B_{kk'} = \sum_{k''} c_{kk''} m_{k''+k'} \quad (56)$$

whereas the corresponding solution of (53) reads (up to a proportionality factor):

$$e(\sigma) = \sum_k a_{k'k} m_k(\sigma) \quad (57)$$

where $a_{k'k}$ is the co-factor (algebraic minor) of $A_{k'k} = \delta_{k'k}^{K^r} + B_{k'k}$ (note that the r.h.s. of (57) is in fact independent of the value of k'). Having found the spinodal (SP) we now turn to the stability condition (ST), eq. (25). Using (51) and writing $\delta\rho_0(\sigma) = \rho(\sigma) e(\sigma)$, eq. (25) can be rewritten ($E = E[\rho]$):

$$\int d\sigma h(\sigma) e^3(\sigma) = 3 \left(\frac{\rho}{E}\right)^2 \left\{ \int d\sigma h(\sigma) e(\sigma) \right\} \left\{ \int d\sigma h(\sigma) e(\sigma) v(\sigma) \right\}^2 + 2 \left(\frac{\rho}{E}\right)^3 \left\{ \int d\sigma h(\sigma) e(\sigma) v(\sigma) \right\}^3 \quad (58)$$

which on choosing $k' = 0$ in (57) and substituting the result into (58) yields:

$$\sum_{k,k',k''} a_{0k} a_{0k'} a_{0k''} m_{k+k'+k''} = 3A^2 (\sum_k a_{0k} m_k) (\sum_{k'} a_{0k'} m_{k'+3n})^2 + 2A^3 (\sum_k a_{0k} m_{k+3n})^3 \quad (59)$$

where, as before, $A = \eta/(1 - \eta m_{3n})$. Finally, in the vdW model eq. (26) is always satisfied because K_4 of (52) is positive definite.

In summary, those thermodynamic states $\{t, \eta, h(\sigma)\}$ for which $\delta^2 f > 0$ are stable while the marginally stable states ($\delta^2 f = 0$) obey the spinodal condition (56). The critical states are stable marginal states, i.e. they must obey both eq. (56) and (59). Note that these equations are algebraic equations involving t , η and moments of the type m_k , $m_{k+k'}$ and $m_{k+k'+k''}$ where $\{k, k', k''\}$ cover the finite set of values $\{0, 3n, l, l+n, l+2n, l+3n\}$ appearing in the excess free-energy.

VII. SOME TYPICAL PHASE DIAGRAMS

Having obtained the basic equations which govern the phase behavior of the present polydisperse vdW-fluid we now consider a few explicit examples. In order to completely characterize a thermodynamic situation we must specify (t, η_0) , the parent phase distribution $h_0(\sigma)$, and the values of (l, n) to be used in (40). In our study we have found no qualitative differences between the two types (SZ or LN) of parent phase distributions considered in

section IV. All features found for one type can be found for the other type by changing the value of the polydispersity index I . On the contrary, the influence of the (l, n) values is much more pronounced, as we now explain.

A. Interactions with size polydispersity only

If we remove the amplitude polydispersity ($l = 0$) and keep only the size polydispersity ($n = 1$) of the interaction potential the present vdW model is governed by the following four moments $\{m_0, m_1, m_2, m_3\}$, i.e. $k = 0, 1, 2, 3$ (see section V). The equations (45-46) governing the binodals constitute then a system of five equations which can be solved numerically and similarly for the C- and S-curves (see (48-49)), as explained in section V. Returning to (42) it is seen that in the present case the effect of the polydispersity ($I \neq 1$) on the repulsions (or excluded volume) is stronger ($\eta \rightarrow \eta m_3$) than its effect on the attractions ($4\eta^2 \rightarrow \eta^2(m_3 + 3m_1 m_2)$) because the moments m_k are increasing functions of $I = 1 + 1/\alpha > 1$ (cf. (36) and (38)). This situation is hence unfavorable to phase separation when compared with the (strictly) monodisperse case ($I = 1$). This can be seen in the phase diagram shown in Fig.2. The result shown corresponds to a SZ parent phase of relatively modest polydispersity index $I = 1.04$ ($\alpha = 25$). Note that at present⁷ it is current practice to consider colloidal dispersions with $I < 1.05$ as (approximately) monodisperse. It is seen in the figure that, when compared to the (strictly) monodisperse case ($I = 1$), the coexistence region is shifted to lower temperatures. As indicated, there exists now a different binodal for each value of η_0 , (instead of the unique binodal when $I = 1$). These binodals are truncated on the high-temperature side and fill the space between the cloud-point(C) and shadow (S) curves. The high-density phase is shifted towards lower densities whereas the low-density phase is only slightly shifted towards higher densities. Note also that the polydispersity distributions, $h_1(\sigma)$ and $h_2(\sigma)$, change with T along the binodals (see Fig.3). The S-curve is situated in the interior of the C-curve and is tangent to the latter at the common maximum of both curves. This common maximum corresponds to a critical point where the two

phases become identical. The binodal through the critical point is the only untruncated binodal. The critical point itself is shifted to lower temperatures and lower densities when compared to the monodisperse case. When increasing the value of I all these shifts increase monotonically without modifying the overall aspect of the phase diagram. As far as we are aware, phase diagrams of this type have not yet been found experimentally but should be observable in suitably prepared colloidal dispersions.

B. Interactions with amplitude polydispersity only

If we remove the size polydispersity ($n = 0$) but keep the amplitude polydispersity ($l \neq 0$, say $l = 1$) the present vdW model is governed by two moments $\{m_0, m_1\}$, i.e. $k = 0, 1$ and eqs. (45-46) reduce to a system of three equations. In this case the polydispersity does only affect the attractions (see, $4\eta^2 \rightarrow \eta^2 \cdot 4m_1^2$, in eq. (42)), a situation which is favorable to phase separation. This is seen in Fig.4 where the phase coexistence region is shown to be shifted to higher temperatures. Note also that the S-curve has moved now to higher densities and also moved partly outside of the interior of the C-curve. As a result the intersection of the C- and S-curves, i.e. the critical point, is encountered now below the temperature (t_m) corresponding to the common maximum of the C- and S-curves. As seen in Fig.4b this allows for a re-entrant behavior of the low density phase. The same behavior is found for any $l > 0$, whatever small. Phase diagrams of this type have been found for some polymeric systems¹⁹.

C. Size and amplitude polydispersity

In a realistic situation we expect $n = 1$ and $l \neq 0$. This increases the number of moments (up to a maximum of six, five for $l = 1$) but it is easily verified that within the present vdW model the attractions are always more strongly affected by the polydispersity than the repulsions and will hence always favor the phase separation. Examples of the resulting phase diagrams are shown in Fig.5. Note that the modifications introduced into the phase

diagram by the amplitude polydispersity (compare Figs.2 and 5) could be used to probe the presence or absence of an amplitude polydispersity in the interaction between the colloidal particles being studied.

VIII. POLYDISPERSITY INDUCED CRITICAL POINTS

In the above we have limited ourselves to the case where only two phases coexist. We have seen that the phase diagram is considerably modified by the polydispersity, in particular in the region of the critical point. When the temperature is lowered, starting from the critical temperature, one expects to encounter a region where three, four, etc. phases coexist. Because only fluid phases are involved we expect the transition from the two-phase to the three-phase region to proceed through a second critical point. Since such a second critical point is absent from the ordinary monodisperse vdW fluid it can be termed polydispersity induced. In the present section we will describe how these polydispersity induced critical points can be found in a systematic way. Critical points can be obtained by following different routes, two of which have already been illustrated in section VII. It was seen there that critical points can be found by either looking for untruncated binodals or for intersections of the C- and S- curves. When the critical region is approximately known these routes are easily executed but this method becomes unpractical when no a priori knowledge about their location is available, as is the case here for all the polydispersity induced critical points. The method to be followed here will therefore be based on the stability criteria of section IIC, as adapted to the vdW case in section VI. When following this route the critical points can be found by looking for intersections of the spinodal (SP) and the stability (ST) curves. In the present context this amounts to look for thermodynamic states (t, η) which, for a given $h(\sigma) = h_0(\sigma)$, satisfy both eq. (56) and (59). In Fig.6 we show how the various routes coincide for the ordinary, high-temperature, vdW critical point. Some of the remaining polydispersity induced critical points obtained from the present route are shown in Fig.7.

It is seen there that when increasing the polydispersity index I , the number of polydis-

polydispersity induced critical points gradually increases. It is also seen that at the same time the region of spinodal instability ($\delta^2 f < 0$ for $\delta\rho(\sigma) = \delta\rho_0(\sigma)$) rapidly invades the high density region of the phase diagram. As a consequence, some of the polydispersity induced transitions and critical points could still be metastable with respect to the solid phases expected to become stable in this high density region.

IX. CONCLUSIONS

In the present study we have presented phase diagrams for fluids composed of spherical particles with a monomodal size distribution. These phase diagrams have been obtained on the basis of the van der Waals approximation for the free-energy of a polydisperse fluid. Interaction potentials with both size and amplitude polydispersity have been considered. It has been found that the largest modifications to the phase diagram of the polydisperse fluid, as compared to its monodisperse counterpart, result from the amplitude polydispersity of the interaction potential. These modifications should already be observable in colloidal dispersions with a relatively small polydispersity index I (e.g. $1.01 \leq I \leq 1.05$). For larger, but still modest values of I (e.g. $1.1 \leq I \leq 1.5$) a second, polydispersity induced, critical point is found signaling the onset of a three phase coexistence. When the value of I is increased still further, high-order coexistences are found but these are located in the high-density region of the phase diagram where the fluid phases considered here are expected to become metastable with respect to the solid phases.

Acknowledgements

M.B. acknowledges financial support from the F.N.R.S.

REFERENCES

- ¹ W.B. Russel, D.A. Saville and W.R. Schowalter, *Colloidal Dispersions*, (Cambridge University Press, Cambridge, 1998).
- ² S. Chandrasekhar, *Liquids Crystals*, (Cambridge University Press, Cambridge, 1992).
- ³ H.G. Elias, *An introduction to Polymer Science*, (VCH Publishers Inc., Weinheim, 1997).
- ⁴ R.T. DeHoff, *Thermodynamics in materials science*, (Mc Graw-Hill Inc., New York, 1993).
- ⁵ R. Aris and G.R. Gavalas, *Philos. Trans. R. Soc. London Ser.A* **260**, 351(1966); J.A. Gualtieri, J.M. Kincaid and G. Morrison, *J. Chem. Phys.* **77**, 521(1982); J.J. Salacuse and G. Stell., *J. Chem. Phys.* **77**, 3714(1982); J.B. Briano and E.D. Glandt, *J. Chem. Phys.* **80**, 3336(1984).
- ⁶ R.J. Hunter, *Foundations of colloid science*, (Clarendon Press, Oxford, 1993).
- ⁷ See e.g., *Observation, Prediction and Simulation of Phase Transitions in Complex Fluids*, (Edited by M. Baus, L.F. Rull and J.P. Ryckaert) (Kluwer Academic Publishers, Dordrecht, 1995); A.P. Gast and W.B. Russel, *Physics Today*, **51**(n° 12), 24(1998).
- ⁸ S. Leroch, G. Kahl and F. Lado, *Phys. Rev. E* **59**, 6937(1999); S.E. Phan, W.B. Russel, J. Zhu and P.M. Chaikin, *J. Chem. Phys.*, **108**, 9789(1998); P. Bartlett, *J. Chem. Phys.* **107**, 188(1997); R. McRae and A.D.J. Haymet, *J.Chem.Phys.* **88**, 1114(1988); J.L. Barrat and J.P. Hansen, *J. Physique* **47**, 1547(1986); and references therein.
- ⁹ P. Bartlett and P.B. Warren, *Phys. Rev. Lett.* **82**,1979(1999); P.B. Warren, *Europhys. Lett.* **46**, 295(1999); J.A. Cuesta, *Europhys. Lett.* **46**, 197(1999); R.M.L. Evans, *Phys. Rev. E* **59** , 3192(1999); R.M.L. Evans, D.J. Fairhurst and W.C.K. Poon, *Phys. Rev. Lett.* **81**,1326(1998); P.B. Warren, *Phys. Rev. Lett.* **80**, 1369(1998); R.P. Sear, *Europhys. Lett.* **44**, 531(1998); P. Sollich and M.E. Cates, *Phys. Rev. Lett.* **80**, 1365(1998); and references therein.
- ¹⁰ R. Lovett and M. Baus, *J. Chem. Phys.*, **111**, 5544(1999); A. Daanoun, C.F. Tejero and M. Baus, *Phys. Rev. E* **50**, 2913(1994); and references therein.
- ¹¹ J.A. Gualtieri, J.M. Kincaid and G. Morrison, *J. Chem. Phys.* **77**, 521(1982).
- ¹² H. Xu and M. Baus, *Phys. Rev. E* **61** , 3249(2000).

- ¹³ M. Baus, *J. Stat. Phys.* **48**, 1129(1987) and references therein.
- ¹⁴ E. Goursat, *A course in mathematical analysis*, vol.3, part2 (Dover Publications Inc., New York, 1964).
- ¹⁵ J.M. Kincaid, R.A. MacDonald and G. Morrison, *J. Chem. Phys.* **87**, 5425(1987); J.M. Kincaid, G. Morrison and E. Lindeberg, *Phys. Lett* **96A**, 471(1983).
- ¹⁶ M.R. Stapleton, D.J. Tildesley and N. Quirke, *J. Chem. Phys.*, **92**, 4456(1990).
- ¹⁷ *Numerical Recipes*, ed. by W.H. Press, B.P. Flannery, S.A. Teukolsky, W.T. Vetterling (Cambridge University Press, Cambridge, 1989).
- ¹⁸ J.A. Cuesta, *Europhys. Lett.* **46**, 197(1999).
- ¹⁹ See e.g., R. Kita, T. Dobashi, T. Yamamoto, N. Nakata and K. Kamide, *Phys. Rev. E* **55**, 3159(1997); N. Clarke, T.C.B. McLeish and S.D. Jenkins, *Macromolecules*, **28**, 4650 (1995).

Figure Captions

FIG. 1. Two examples of the Schulz-Zimm (SZ) (solid lines) and log-normal (LN) (dotted lines) parent phase distributions, $h_0(\sigma)$, considered in this work (see (34-37)). The values of the polydispersity index (I) are, $I = 1.04$ and $I = 4/3$ (as indicated). It is seen that for the values of I considered here ($1 < I < 2$) these two distributions are rather similar. In particular, both are very small for the larger σ -values. Note also that the average value of σ ($m_1^{(0)} = 1$) does not coincide with the value of σ for which $h_0(\sigma)$ reaches its maximum.

FIG. 2. An example of a phase diagram (in (a) the reduced temperature ($t = k_B T/\epsilon(1, 1)$)-reduced density ($\eta = \rho v(1)$) plane and (b) the reduced pressure ($\bar{p} = pv(1)/\epsilon(1, 1)$)-reduced temperature (t) plane) for the SZ parent phase distribution ($I = 1.04$) shown in Fig.1 and the vdW-model ($l = 0, n = 1$) with only a size polydispersity. For comparison the monodisperse phase diagram ($I = 1$) (dashed line) has also been included. Shown are, the C-curve (full dots), the S-curve (open dots), and three binodals (full lines) for resp. $\eta_0 = 0.15$, $\eta_0 = 0.35$ and $\eta_0 = \eta_{crit} = 0.2852$ together with a tie line (dotted lines of (a)) corresponding to the upper temperature of coexistence (the lowest tie line shown belongs to the $\eta_0 = 0.15$ binodal). The critical point is indicated by a square (filled for $I = 1.04$ and open for $I = 1$). Note also that in the $p - t$ diagram (b) the C- and S-curves coincide (with $\eta_1 < \eta_2$ on the upper branch and $\eta_1 > \eta_2$ on the lower branch).

FIG.3. Evolution of the polydispersity distributions of the coexisting phases, $h_1(\sigma)$ and $h_2(\sigma)$, with the temperature along the critical binodal ($\eta_0 = \eta_{crit} = 0.2852$) of Fig.2. Shown are : $h_1(\sigma)$ (full line, $t = 0.9$; dash-dot line, $t = 1.12$) and $h_2(\sigma)$ (dotted line, $t = 0.9$; full dots, $t = 1.12$).

FIG.4. The same as Fig.2 but for the vdW-model ($l = 1, n = 0$) with amplitude polydispersity only. The case shown corresponds to a SZ parent phase distribution with $I = 1.02$. The three binodals shown correspond to $\eta_0 = 0.25$ (outer), $\eta_0 = 0.45$ (inner) and the critical binodal $\eta_0 = \eta_{crit} = 0.346$ (middle). Note that in the $p - t$ diagram the critical point corresponds to the maximum of the pressure but not to the maximum of the temperature (t_m) for coexistence. The latter can also be seen in the $t - \eta$ diagram. This implies a re-entrant behaviour for $t_{crit} < t < t_m$.

FIG.5. The same as Fig.2 but for the vdW-model ($l = 1, n = 1$) with both size and

amplitude polydispersity. The case shown corresponds to a SZ parent phase distribution with $I = 1.01$. The three binodals shown correspond to $\eta_0 = 0.25$ (outer), $\eta_0 = 0.4$ (inner) together with the critical binodal $\eta_0 = \eta_{crit} = 0.3338$ (middle). Note that this phase diagram is globally similar to the one of Fig.4 but shifted to higher temperatures although the value of I is smaller here. The phase diagrams are very sensitive to the total amount of polydispersity present, i.e. to the values of l and n .

FIG.6. The critical point shown in Fig.5 as determined by three different routes : 1) the maximum of the untruncated critical ($\eta_0 = \eta_{crit}$) binodal(B), 2) the intersection of the C- and S-curves and 3) the intersection of the spinodal (SP) and stability (ST) curves. Note that the SP-curve is tangent to the C-curve at the critical point ($t_{crit} = 1.2620$, $\eta_{crit} = 0.3338$).

FIG. 7. Evolution of the number of critical points for a vdW fluid with both size and amplitude polydispersity ($l = 1$, $n = 1$) and a LN parent phase distribution of increasing polydispersity ((a): $I = 1.1$, (b): $I = 4/3$). Similar results can be obtained for the SZ distribution. The critical points (full dots) correspond to the intersection of the SP (full line) and the ST (dashed line) curves. Note that when I increases the number of critical points increases (one for $1 < I < 1.09$, two for $1.09 < I < 1.5$, etc.) while at the same time the spinodal region invades the high density portion of the reduced temperature (t)-average packing fraction ($\eta^* = \eta m_3$) plane (here $m_3 = I^3$ is the third moment of the LN distribution).

Fig. 1 , Bellier-Castella et al., JCP

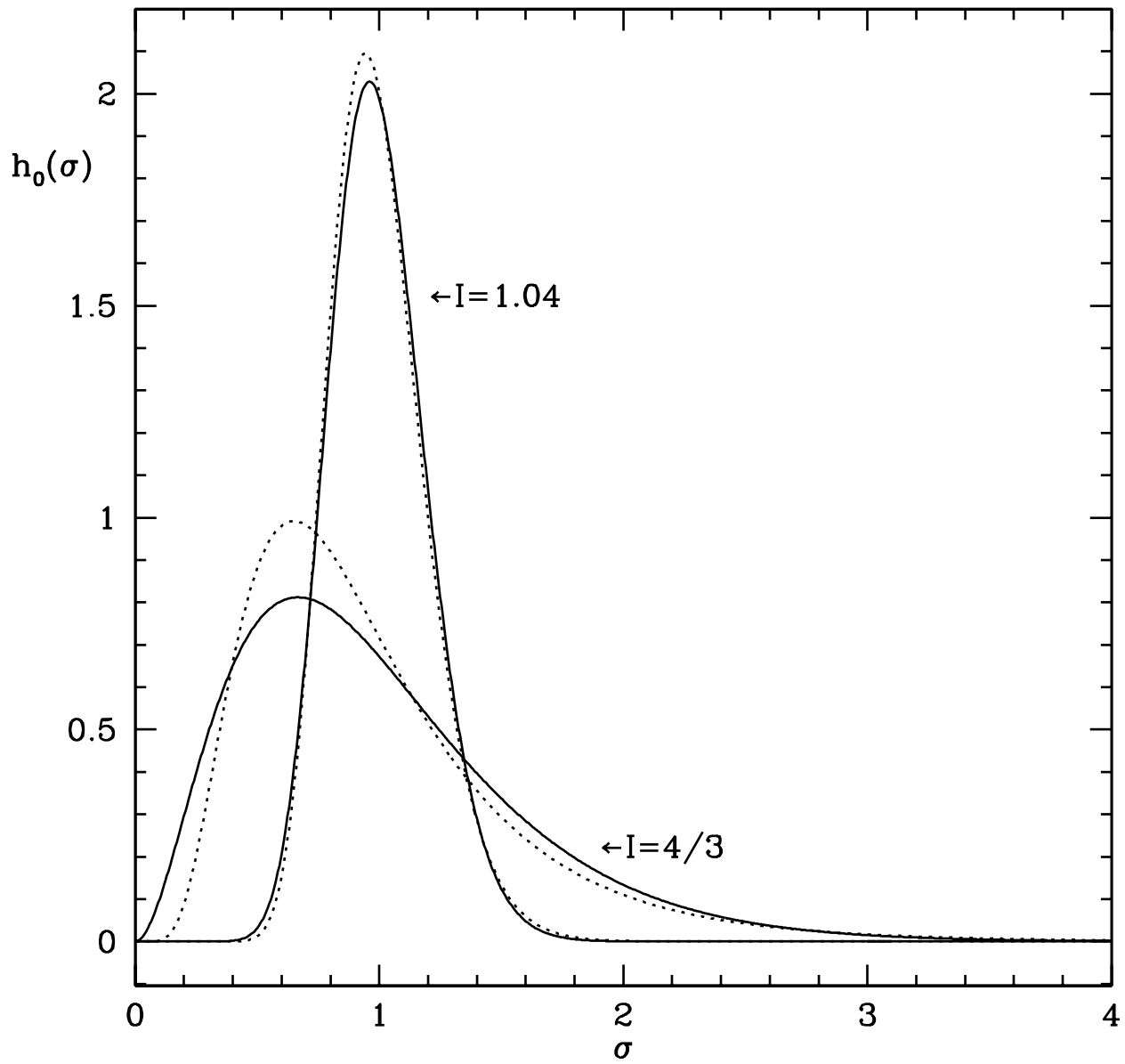


Fig. 2a , Bellier-Castella et al., JCP

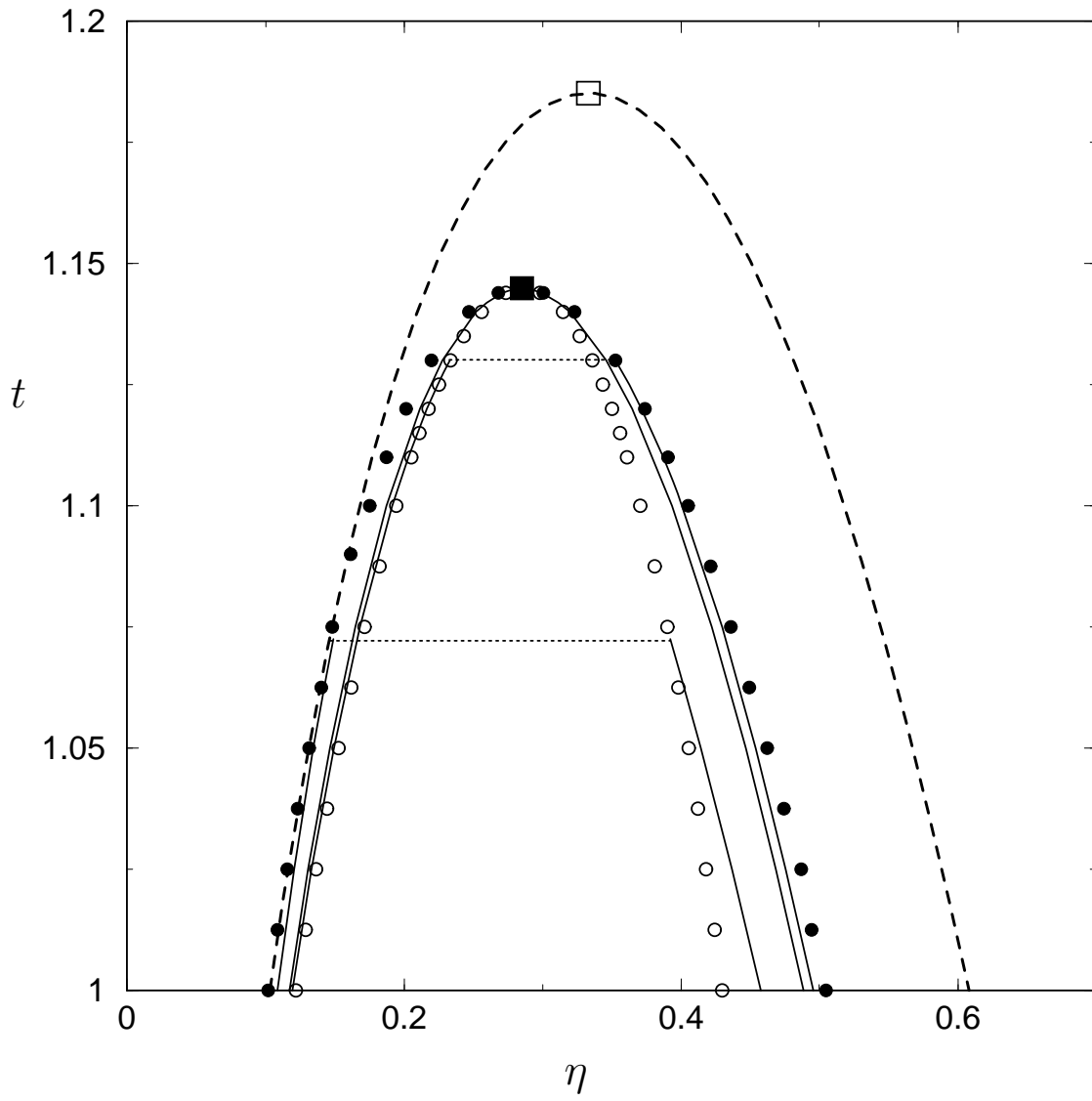


Fig. 2b , Bellier-Castella et al., JCP

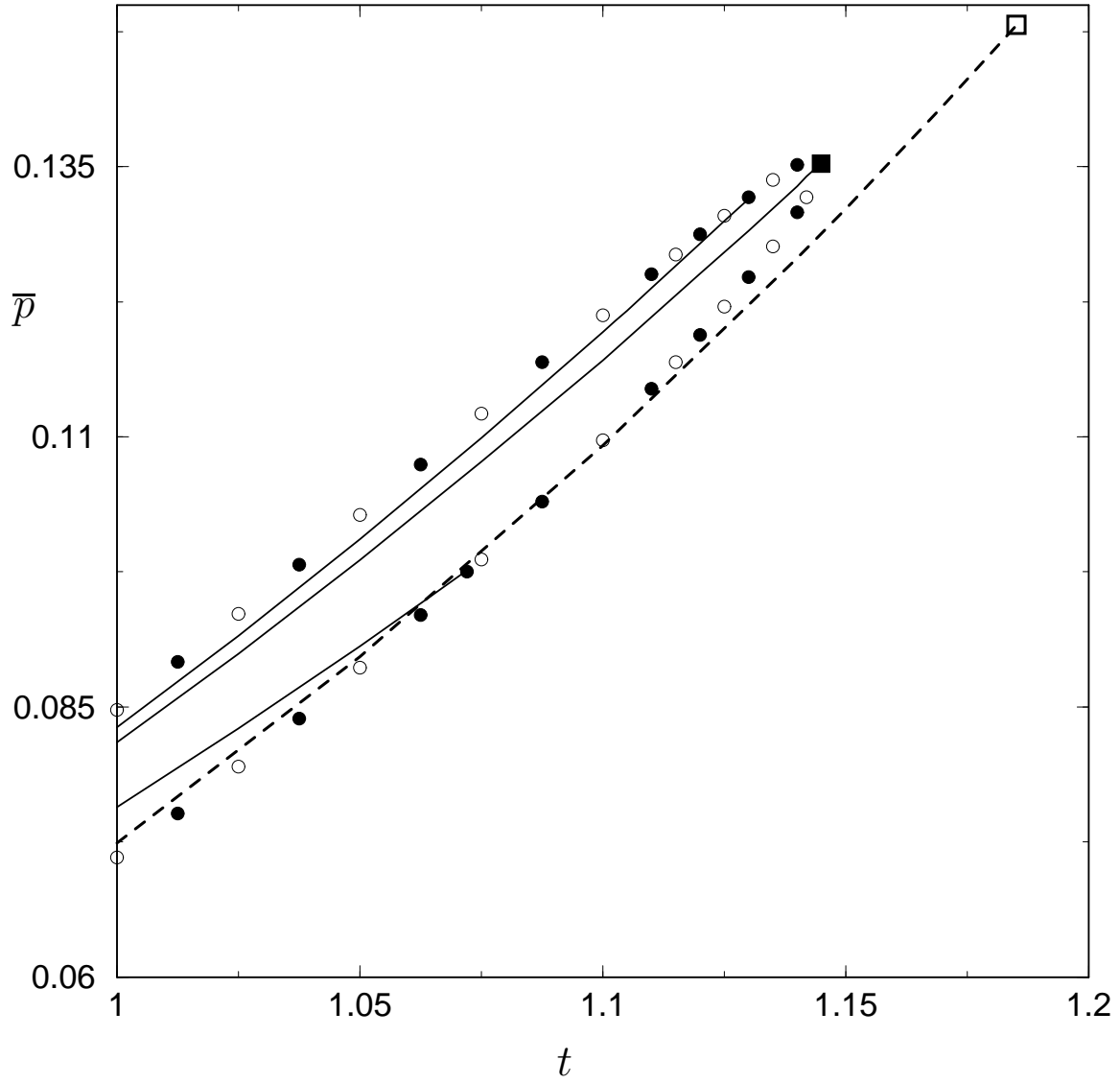


Fig. 3 , Bellier-Castella et al., JCP

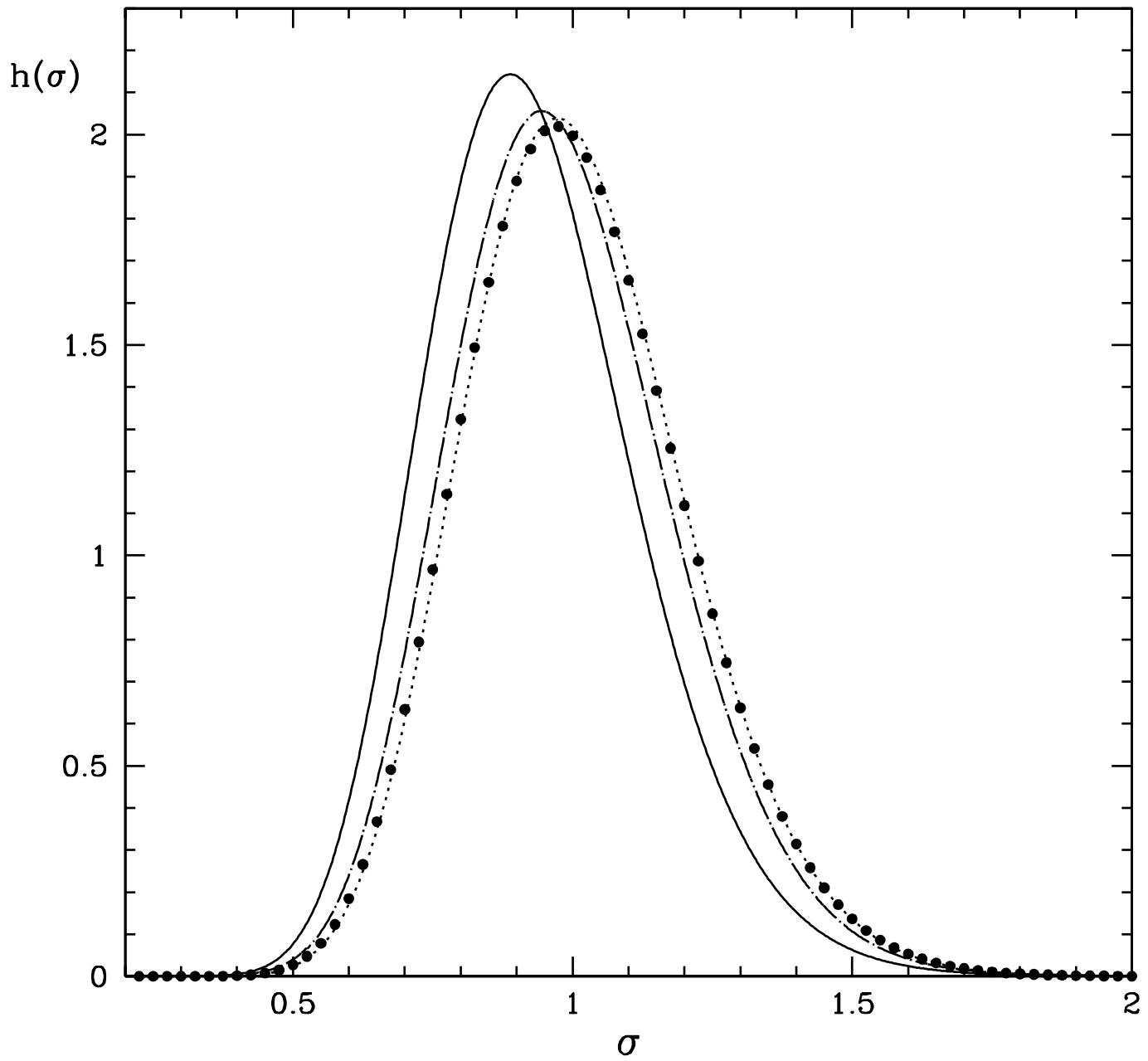


Fig. 4a , Bellier-Castella et al., JCP

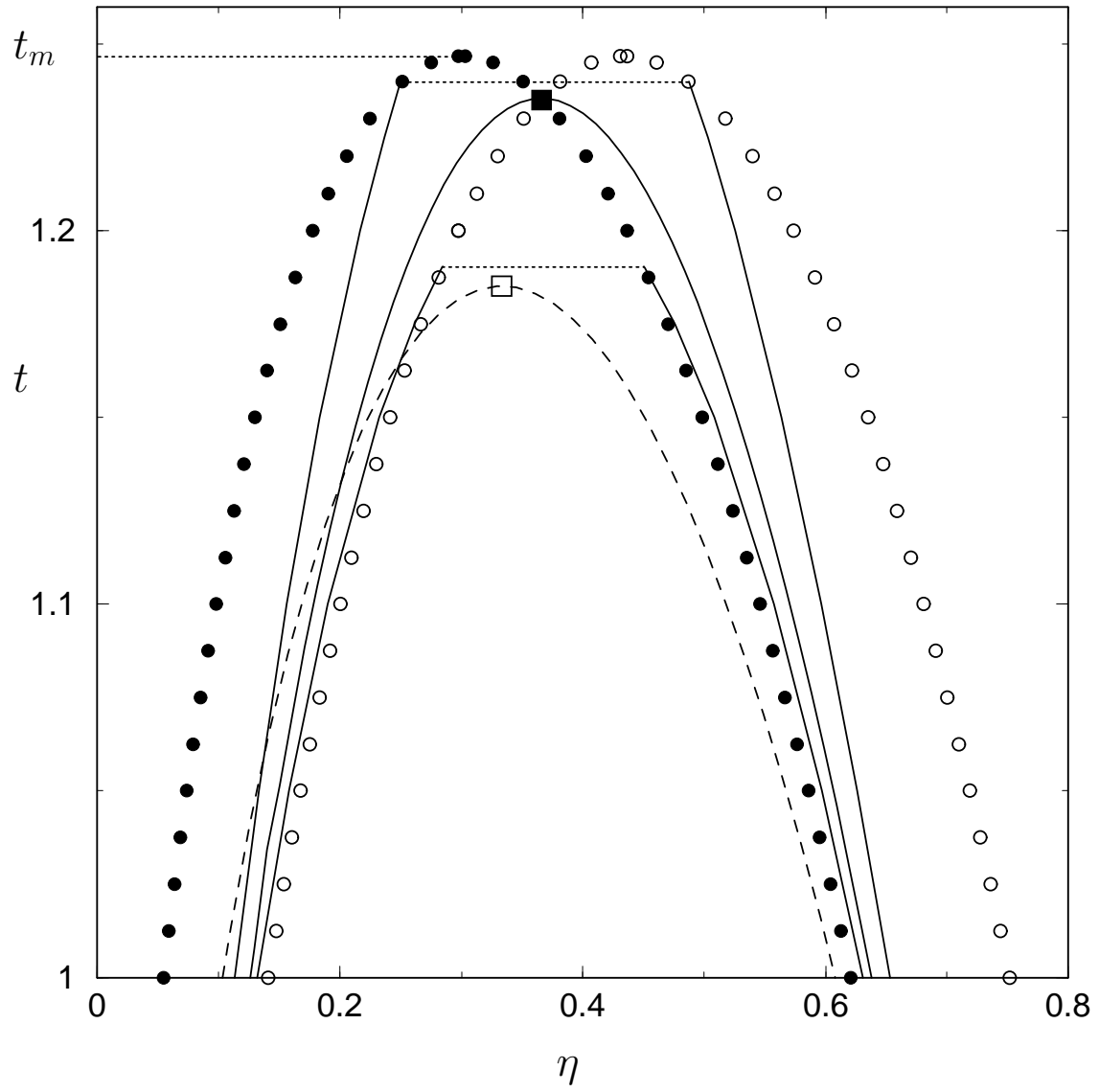


Fig. 4b , Bellier-Castella et al., JCP

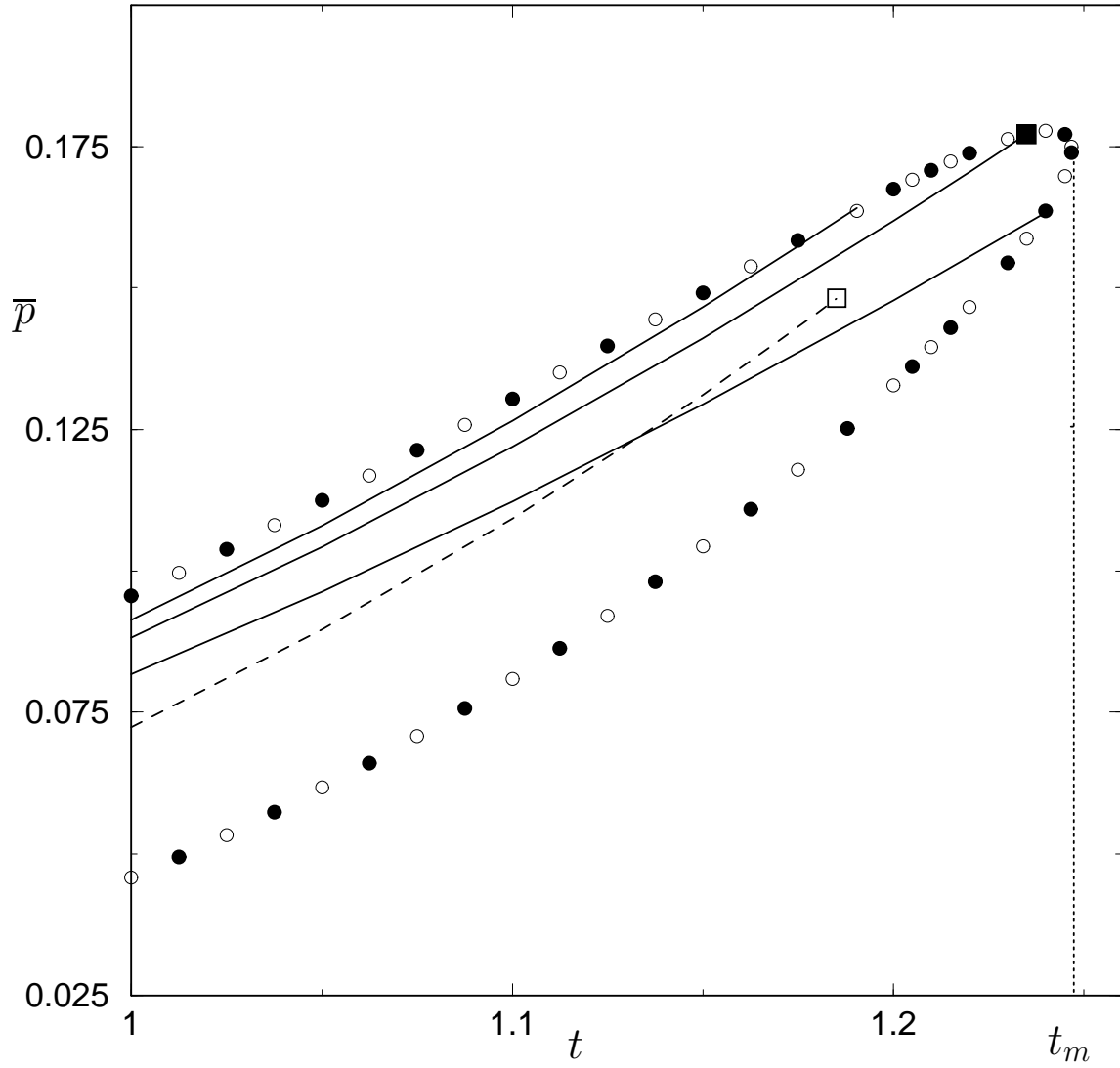


Fig. 5a , Bellier-Castella et al., JCP

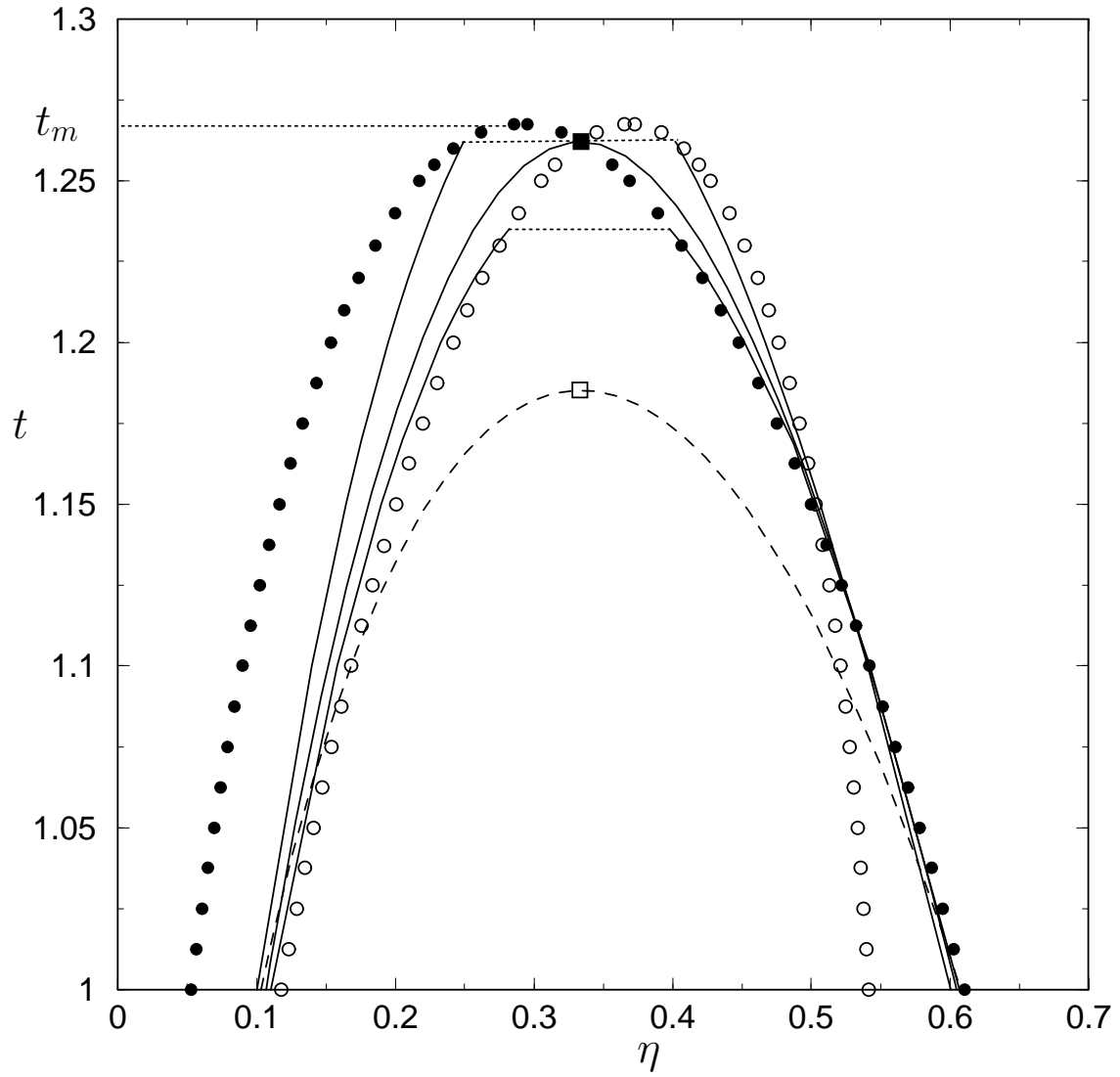


Fig. 5b , Bellier-Castella et al., JCP

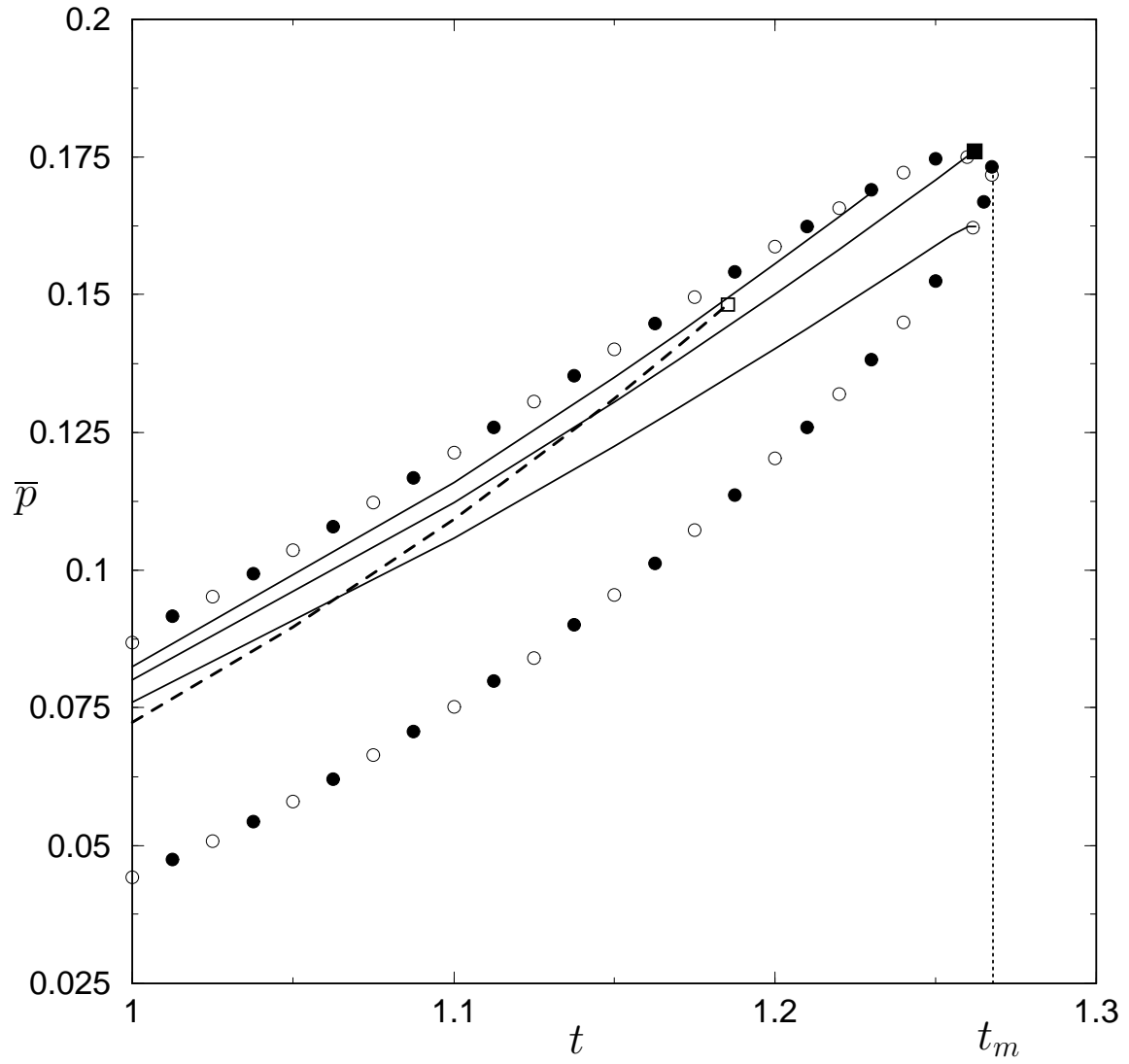


Fig. 6 , Bellier-Castella et al., JCP

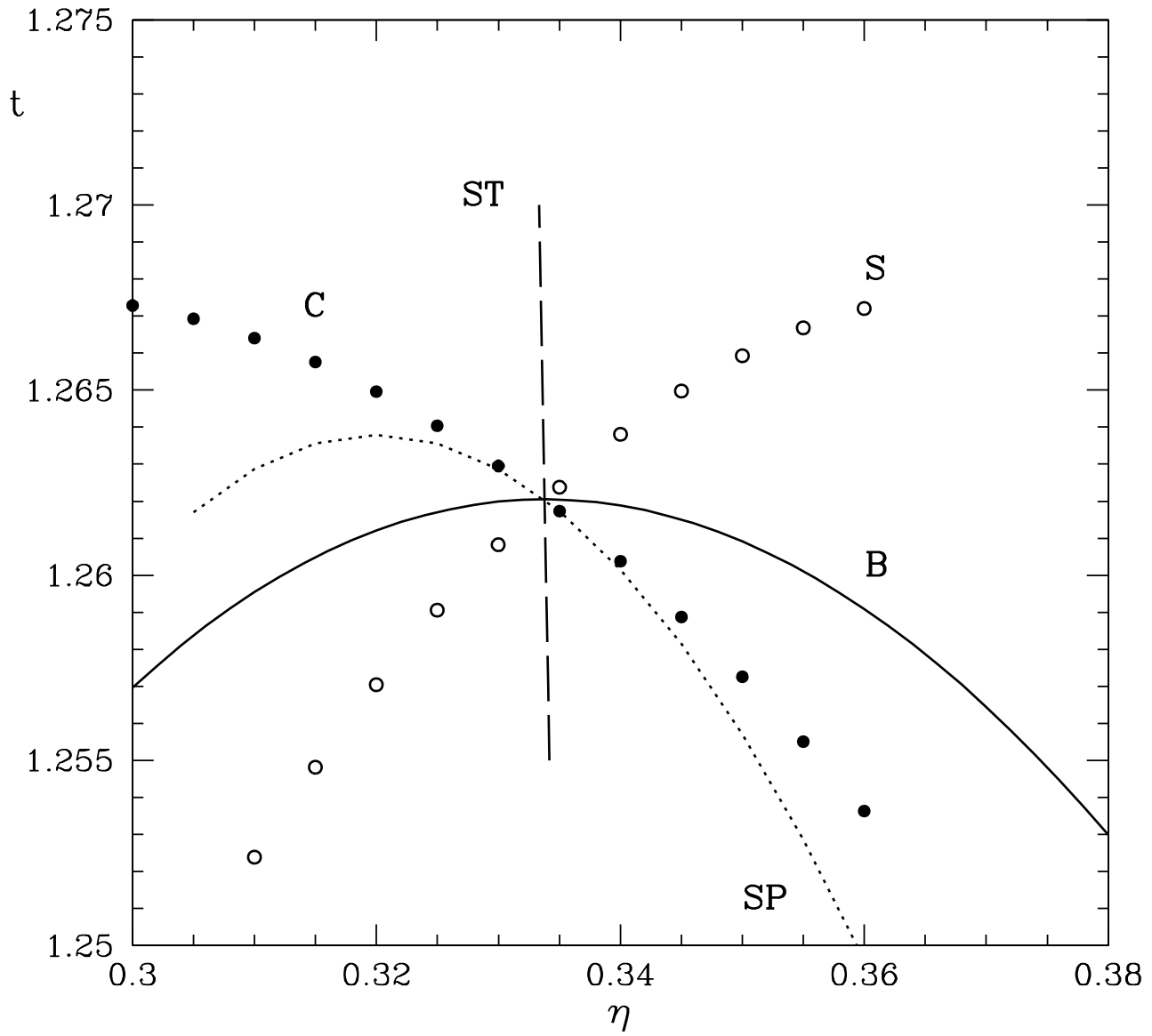


Fig. 7 , Bellier-Castella et al., JCP

